Design and Realization of a Non-Destructive Testing Device Operating on Eddy Current Principle

Cung Thanh Long*, Bui Dang Thanh, Dao Duc Thinh, Nguyen Van Tung
Hanoi University of Science and Technology, No.1, Dai Co Viet, Hai Ba Trung, Hanoi, Viet Nam
Received: June 06, 2016; accepted: June 9, 2017

Abstract

This paper presents a design of a non – destructive testing device using eddy current technique. This device has a sinusoidal excitation source consisting of 4 frequencies which developed to operate with double-function eddy current sensors. The testing results are displayed on a black and white graphic LCD as a function of sensor's output voltage to testing position, and user's evaluation is based on the shape of this signal. Experiments on several kind of tested specimen show that this device operates stably and can detect small surface or under-surface cracks.

Keywords: eddy current, non-destructive testing, surface crack, under-surface crack

1. Introduction

Eddy current (EC) technique is one of the most widely used non-destructive testing/evaluation techniques. The principle of this technique consists in inducing EC inside the inspected structure, for example by means of a coil and, on the other hand, in sensing the response of the structure to the EC excitation, for example through the resulting impedance variations at the ends of the inducting coil (eddy current sensor), as they reflect the local (either electrical or geometrical) characteristics of the target. Concretely, the basic configuration of an eddy current sensor consists of a conductive coil stimulated by an alternating (sinusoidal or pulsed) electric current. Under the excitation current, it appears an alternating magnetic field around the coil, called excitation magnetic field. Approaching a conductive specimen to this field, circular electric currents (eddy currents) will appear and concentrate mostly near the surface of the specimen. These currents, by their turn, create an induction magnetic field which is opposite to the excitation one. As consequence, the total magnetic field through the coil which consisting of the excitation and induction fields will be a function of many parameters. It depends on the distance from coil to tested structure, on the nature and condition of the object to be examined (such as thickness, surface shape, internal cracks, material of the object), as well as on the frequency of excitation source. By measuring directly this field, or through related quantities such as output voltage, impedance, or normalized impedance [1] of the sensor, affections of the above parameters can be realized.

The eddy current technique is widely used to detect cracks on the surface or sub-surface of metallic structures [2]; to detect the change in electrical conductivity [3], the change in thickness of tested objects, or the change in thickness of non-metallic coating on a tested structure [4]. Moreover, a lot of approaches are proposed to solve the problem of sizing cracks, measuring thickness of massive or multilayered structures [5]. Nowadays, non-destructive testing (NDT) devices based on eddy current technique have been commercialized and widely used in the world. For this type of device, the testing results are almost displayed as graphical indications. On the shape of graphs, characteristics of inspected structures can be qualitatively evaluated. However, to our knowledge, in our country, till recently, there are not published researches on the design and fabrication of an EC NDT device.

In this paper we present a design of a prototype of EC NDT device, which can detect surface cracks, under surface cracks or under coating cracks on a conductive specimen. In section 2 of the paper, we report on the design of device hardware. Section 3 is focus on the presentation of solutions for signal processing and display. Section 4 presents experiment setups for device testing and some discussions on the obtained results. Finally, our conclusions are presented in the section 5.

* Corresponding author : Tel (+84)963 95 88 54
Email : long.cungthanh@hust.edu.vn

2. Hardware design

The hardware of the device consists of three main parts: excitation source, sensor and processing unit. The sensor is an air cored double function eddy current sensor, which is excited by sinusoidal voltage source, with 4 different excitation frequencies. The processing unit plays a role of signal amplification and standardization. In addition, it manages the display of testing results on the screen of the device. The excitation source and the processing unit are integrated in the device body, while the sensor is housed in a cylindrical frame with noise-isolating cover. The device operates on 9V battery power source, ensuring the mobility and the flexible usability in actual measurement conditions.

2.1. Sinusoidal excitation source

In this study, the integrated circuit XR2206 of EXAR is used to generate sinusoidal signals. It allows to adjust both the amplitude and frequency of the output signal.

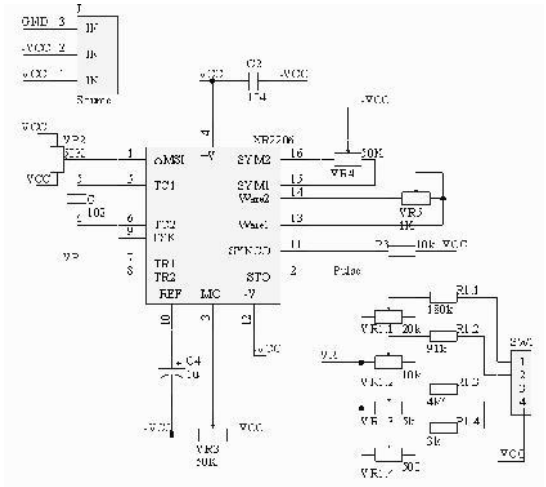

Fig. 1. Circuit of sinusoidal signal generation using XR2206.

Fig. 1 shows the design of a sinusoidal excitation source using the XR2206. The signal generated on pin 2 has a frequency determined by the value of capacitor C (connected between the pins 5 and 6) and the value of resistors selected from the pins which connected to the switch SW1. In fact, one of these resistors is selected via a rotary switch connected between SW1 and the supplied source ($-V_{CC}$). If the resistor connected to pin TR1 is called R, the frequency of output signal is determined by (1)

$$f = \frac{1}{RC} \qquad (1)$$

Following equation (1) we use four sets of resistors (R1.1 + VR1.1), (R1.2 + VR1.2), (R1.3 + VR1.3), (R1.4 + VR1.4) as indicated in Fig. 1, in order to get four excitation frequencies of 5 kHz, 10 kHz, 100 kHz and 200 kHz.

The sinusoidal signal at the output of the integrated circuit XR2206 is passed through an amplification circuit as shown in Fig. 2. The used amplifier is LF356 which can operate with high frequency input signals. In this circuit, IC1 is used to immobilize the signal from the previous circuit, IC2 is used to amplify the signal, and IC3 is used to immobilize the amplified output voltage. This design allows us to have a stable excitation source.

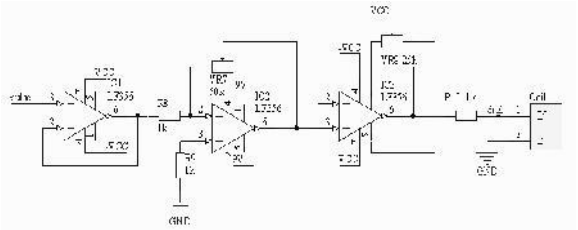

Fig. 2. Circuit of sinusoidal signal amplification.

2.2. Eddy current sensor

During the design and realization process, sensor dimensions are considered based on two limited conditions. For the coil, we needs to have a sufficient number of wire turns, and a large enough diameter of wire. Once this constraint is satisfied, the coil can be used with a large excitation current to generate a strong excitation magnetic field. As result, a high density of eddy currents which penetrating into the tested structure can be obtained. At the same time, the sensor must be small enough to eliminate boundary effects when testing on small surface areas.

In this study, we fabricated and tested a number of different sensor prototypes. These prototypes are different on the shape and the number of wire loops. However, they are made to use on surfaces which have at least 50 mm long in each dimension. The type of sensor which has small enough dimensions, large enough number of wire turns, simple structure, and easy to implement will be chosen.

Concretely, three air cored sensor types are tested to compare their sensitivity. It includes:

- A flat and square coil features 30 turns, and an outer size of 30mm x 30mm
- A flat and round coil features 30 turns and an outer diameter of 30mm
- A cylindrical coil features 30 turns, outer diameter of 15mm, inner diameter of 13mm, and 5mm high.

These sensors are tested with a 10mA current source. The frequency of this excitation source varies from 0 ÷ 30 kHz, with each changing step of 2 kHz.

Let U_0 and U_m are the voltages at the output of the sensor when placed in the air and on the tested specimen, respectively. The value of δU which is defined by (2):

$$\delta U = (U_0 - Um) / U_0 \quad (2)$$

is the quantity used to compare the sensitivity of the sensors. The comparison results are shown in Fig. 3.

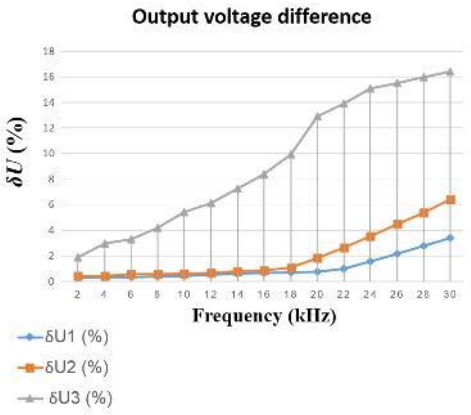

Fig. 3. Comparing the sensitivity of sensors: δU1 - flat square sensor; δU2 - flat round sensor; δU3 - cylindrical sensor.

It can be seen that, with the same wire turns, the same sensor size, and the same testing conditions, the variation of output voltage measured on the air cored cylindrical sensor is greater than that of two flat types. It means the sensitivity of the cylindrical sensor is higher. Moreover, thanks to the cylindrical structure, it is possible to increase the number of wire turn without increasing the diameter of sensor. Because of these advantages, the cylindrical sensor is chosen to use. For our testing device developed in this study, we fabricated a sensor featuring 100 turns, with an outer diameter of 15 mm, an inner diameter of 10 mm, and a height of 12mm. The sensor is housed in a non-conductive tube. The plastic case, sensor and connecting cable form the probe of NDT device. This probe is connected to device body via a 3.5mm audio jack as shown in Fig. 4.

2.3. Circuit for amplification and standardization of sensor signal

The output voltage of EC sensor is very small, only at tens of millivolts. This voltage is amplified and converted into a direct signal by using a circuit as shown in Fig. 5. This circuit consists of two Op Amp LF356 connected in series, with the function of signal amplification and standardization. The output signal is then passed to an embedded analog to digital converter in a microcontroller.

Fig. 4. Probe of EC non-destructive testing device

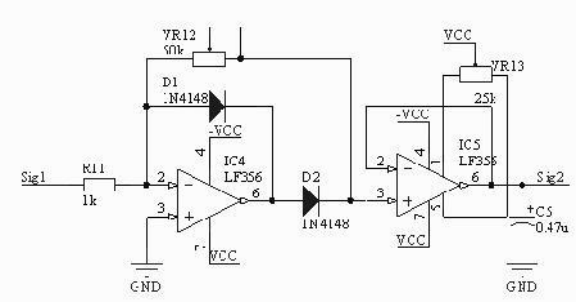

Fig. 5. Amplification and standardization circuit for output signal of EC sensor.

Fig. 6. The front of EC NDT device.

In this preliminary research, we use an Atmega328 microcontroller as the central processing unit. It receives and processes signals (after amplification and standardization) from EC sensor. After being processed, these signals are sent to the LCD 12864ZW for display.

All mentioned functional circuits and battery cavity are packed together in a rectangular case, and served as the device body. Fig. 6 shows the layout in front of it.

3. Software solution for display of tested results

The algorithmic flowchart of the solution for display of tested results is shown in Fig. 7.

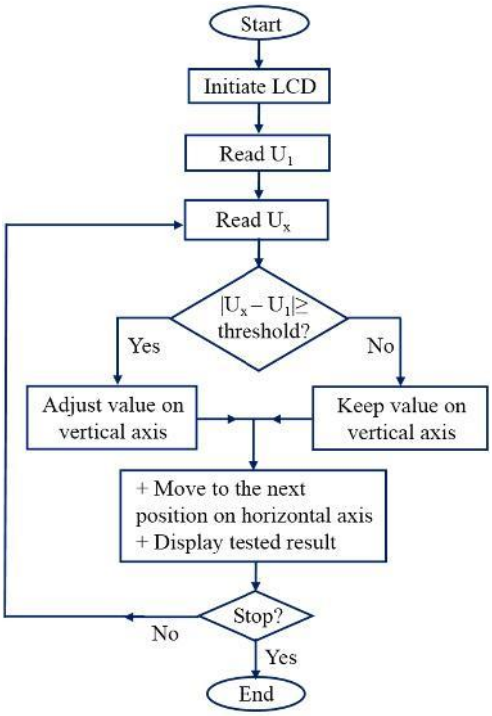

Fig. 7. Flowchart for display solution.

At the time the device is activated, LCD is initiated and the original coordinates are displayed. When EC sensor starts to be placed on the surface of the tested structure, the output voltage U_1 of the sensor is recorded and stored as a reference for displaying the tested results.

Moving the probe to the next test position, the voltage obtained is U_x. Then U_x is compared to the reference U_1, which calculates the deviation (3)

$$\Delta U = | U_x - U_1 | \quad (3)$$

If ΔU is not greater than the defined threshold, this tested result will be displayed on LCD with the same height to reference. In contrast, the height will be determined corresponding to the value of ΔU. For each new test position, the value on the horizontal axis increases by 1 unit. So the tested results are displayed continuously over time from the left to the right on the screen of NDT device. When the right side of LCD is reached, the display will back to run from the original point on the left.

Defects, once detected, will be observed on the screen as a pulse with a higher amplitude than the background. The width and depth of defects have the relationship to the shape of pulses displayed on the LCD.

4. Device testing and discussions

Our developed device was tested on two aluminum alloy specimens. The defects on these samples are accurately created by CNC machine. Their position and size are illustrated in Fig. 8 and Fig. 9.

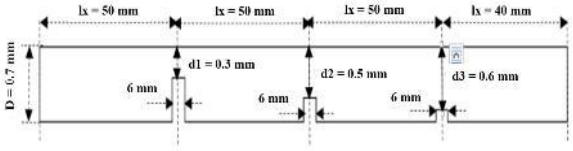

Fig. 8. The first testing sample.

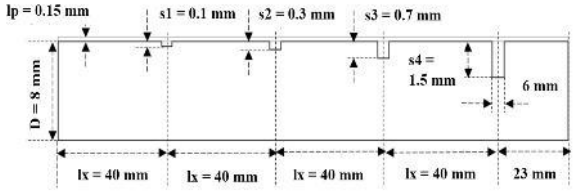

Fig. 9. The second testing sample.

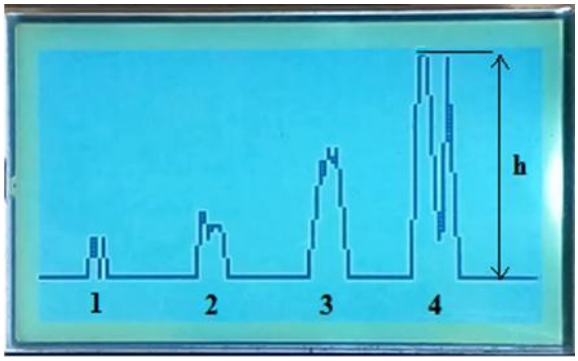

Fig. 10. Tested results on the second sample at the frequency of 200 kHz.

The first sample is used to test the ability of device for under-surface crack detection. The second sample is covered with a thin polycarbonate layer featuring a thickness of 0.15mm. This sample is used to test the usability of device for surface crack detection, in case of having a lift-off between probe and tested structure, or in case of surface cracks located under a thin non-metallic coating.

Tested results show that the detection ability of device depends largely on the excitation frequency. It can be realized that the size and depth of defects are related to the width and height of corresponding pulse displayed on the screen of device (as indicated in Fig. 10). As a summary, the detection capability of the device is listed in Table 1 and Table 2 for all case of test implemented on the first and the second sample, respectively.

Table 1. Tested results conducted on the first testing sample

Excitation frequency	Under-surface defects can be detected
5 kHz	d_1, d_2, d_3
10 kHz	d_1, d_2
100 kHz	Not yet detected
200 kHz	Not yet detected

Table 2. Tested results conducted on the second testing sample

Excitation frequency	Surface-crack depth can be detected
5 kHz	s_2, s_3, s_4
10 kHz	s_2, s_3, s_4
100 kHz	s_1,s_2, s_3, s_4
200 kHz	s_1,s_2, s_3, s_4

With experiments conducted on the first sample, the device is only able to detect cracks that located at a distance which is smaller than 0.7mm from the tested surface (when using two low excitation frequencies 5 kHz and 10 kHz). At two frequencies of 100 kHz and 200 kHz, because of shallow penetration of EC, then the device cannot detect any crack with the distance of 0.3mm to 0.7mm from surface of sample (Table 1).

For the second sample, all cracks are on the surface of specimen with the same width but different depth. When using two excitation frequencies of 5 kHz and 10 kHz, the device cannot detect crack featuring a depth of 0.1mm. This can be explained that due to its small depth, the crack did not significantly affect to the induction magnetic field of eddy currents, leading to the small sensor's output and therefore the device could not detect it. At two higher excitation frequencies (100 kHz and 200 kHz), eddy current density is concentrated almost at the surface of tested specimen, so that all surface cracks cause significant change in induction magnetic field of EC sensor and therefore they are detected. Figure 10 shows that the greater the depth of crack, the higher the ability of detection (as indicated by the height *h* of indicated pulse on the screen).

The tested results are perfectly consistent with theory. Using lower excitation frequencies, the device can detect cracks located deeper in tested specimens. It also indicates that higher excitation frequencies are more sensitive to surface defects. However, the posed sensitive threshold of device should be studied to adjust in order to improve the capability of detecting shallow surface cracks.

5. Conclusion

In this study, we have developed a prototype of non-destructive testing device using eddy current technique. The device is designed to operate with double function air cored absolute EC sensor on four excitation frequencies. It can detect under-surface cracks located at the distance of less than 1 mm from testing surface. For surface cracks, the device can detect defects featuring a depth of greater than 0.1 mm.

The developed device has only the ability of answering if exist or not exist defects, based on the display of the output voltage deviation of EC sensor. To our future works, the device will be upgraded in the direction of adding display mode (display in the normalized impedance plane); improving hardware device to use both double function and separate function sensor; adjusting the sensitive threshold of the device to improve the accuracy of shallow crack detection and eliminating the impact of scratches on the test surface.

Acknowledgement

This research is funded by Vietnam National Foundation for Science and Technology Development (NAFOSTED) under grant number 103.99-2014.31.

References

[1] T. L. Cung, P. Y. Joubert, and E. Vourch, "Eddy current evaluation of air–gaps in aeronautical multilayered assemblies using a multi-frequency behavioral model," Measurement, vol. 44, no. 6, (2011) pp. 1108–1116.

[2] X. Li, B. Gao, W. L. Woo, G. Y. Tian, X. Qiu, and L. Gu, "Quantitative Surface Crack Evaluation Based on Eddy Current Pulsed Thermography," IEEE Sens. J., vol. 17, no. 2, (2017) pp. 412–421.

[3] W. E. Deeds and C. V. Dodd, "Determination of Multiple Properties with Multiple Eddy-Current Measurements," Int Adv Nondestr Test U. S., vol. 8, (1981).

[4] H. Ping-jie and W. Zhao-tong, "Inversion of thicknesses of multi-layered structures from eddy current testing measurements," J. Zhejiang Univ.-Sci. A, vol. 5, no. 1, (2004) pp. 86–91.

[5] E. Vourc'h, P.-Y. Joubert, G. L. Gac, and P. larzabal, "Nondestructive evaluation of loose assemblies using multi-frequency eddy currents and artificial neural networks," Meas. Sci. Technol., vol. 24, no. 12, (2013) p. 125604.